ON A COINCIDENCE MEASUREMENT IN THE YAGUAR NN-EXPERIMENT

B. E. Crawford,[1] E. I. Sharapov,[2] S. L. Stephenson,[1]

[1]Gettysburg College, 300 N. Washington Street, Gettysburg PA 17325, USA
[2]Joint Institute for Nuclear Research, 141980 Dubna, Russia

Abstract

A hypothesized improvement for the signal-to-noise ratio in the DIANNA nn-scattering experiment at the pulsed YAGUAR reactor would be to measure coincidences between the existing detector located below the scattering volume and an additional detector equidistant but above the scattering volume. Here we determine and compare the relative size of the coincidence count rate with the single detector count rate. We present an analytical estimate and results of Monte Carlo modeling with the modified code PZSIM [1] previously developed to calculate the detector counts and neutron spectra after nn-scattering. Results suggest a coincidence efficiency of 10^{-5} to 10^{-6} relative to a single detector geometry, where the range of values depends on the detection options. This coincidence rate is too low to be statistically informative.

1 Introduction

Motivated by a desire to understand charge symmetry breaking of the nuclear force, the neutron-neutron scattering length, a_{nn}, has been actively pursued for several decades [2]. Current values of a_{nn} come from the indirect measurements of the ${}^2H(\pi^-, \gamma n)n$, ${}^2H(n, nn)p$, ${}^2H(n, np)n$ reactions. Current values from these experiments are $a_{nn} = -18.6 \pm 0.3$ fm [3], $a_{nn} = -18.8 \pm 0.5$ fm [4], and $a_{nn} = -16.1 \pm 0.4$ fm [5], respectively.

To help resolve the current discrepancies between these values, the Direct Investigation of a_{NN} Association (DIANNA) is using the aperiodic pulsed Yaguar reactor at Snezhinsk, Russia, which can produce pulsed neutron fluxes of $\Phi \simeq 10^{18}/\text{cm}^2\text{s}$ [6] to directly measure a_{nn} from neutron-neutron scattering with an accuracy of a 3% [7]. The experimental nn-setup is shown schematically in Fig. 1. The original reactor through channel has been modified with a CH_2 cylindrical moderator. A 12-m evacuated, collimated flight path with neutron detector has been assembled below the reactor itself. The detector diameter is 20 cm, with a solid angle of 3×10^{-6} in 4π and is nearly 100% efficient to thermal neutrons. Reducing the neutron background and correcting the nn-scattering signal for residual background counts is the primary experimental challenge; a ^{10}B "back wall" absorber and a special collimator system have been installed for this purpose. With these in place, extensive modeling and test measurements have shown that a signal-to-background ratio of three is achievable [8]. Nonetheless, any ideas for improving this ratio warrant consideration.

One such suggestion has been to replace the ^{10}B "back wall" absorber with a second detector in order to measure coincidences between neutrons that scatter back-to-back

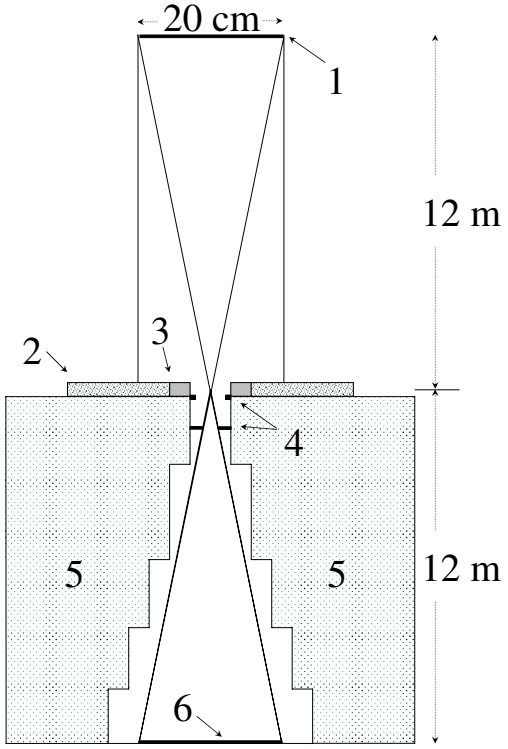

Figure 1: Schematic of experimental setup (not to scale). 1 – ^{10}B back wall or upper neutron detector for coincidence measurement, 2 – reactor core, 3 – polyethylene moderator, 4 – collimators with a minimal apperture of 3 cm, 5 – shielding, 6 – main neutron detector of with 20-cm diameter.

toward and away from the main detector. We describe here analytic estimates and Monte-Carlo modeling of the coincidence rate in that scenario.

2 Analytic estimate

Fig. 2 shows the geometry for the analytical calculations of the nn experiment. Neutrons leave source points Q_1 and Q_2 with velocity vectors $\vec{v}_1$ and $\vec{v}_1$ and collide at point P. The vector $\vec{v}_{cm}$ is the center of mass velocity for these two neutrons. The final velocities of interest $\vec{v}_f$ lie in the detector solid angle $d\Omega_{det}$ along the z-axis. The opening angle of $d\Omega_{det} = \theta_{det}$, has a value of about 1°. To simplify the present analytical calculations we assume that all neutrons have the same speeds v and that vectors v_{cm} are distributed uniformly in space. The final speeds v_{1f} and v_{2f} are calculated as

$$\begin{aligned} v_{1f}^2 &= v_{cm}^2 + (v^*)^2 + 2v_{cm}v^*\cos\theta^* \\ v_{2f}^2 &= v_{cm}^2 + (v^*)^2 - 2v_{cm}v^*\cos\theta^*, \end{aligned} \tag{1}$$

and their cosines with respect to the direction of $\vec{v}_{cm}$ are

$$\begin{aligned} \cos\theta_{1f} &= (v_{cm} + v^*\cos\theta^*)\,/\sqrt{v_{cm}^2 + (v^*)^2 + 2v_{cm}v^*\cos\theta^*} \\ \cos\theta_{2f} &= (v_{cm} - v^*\cos\theta^*)\,/\sqrt{v_{cm}^2 - (v^*)^2 + 2v_{cm}v^*\cos\theta^*}. \end{aligned} \tag{2}$$

The angle θ_{1f} is the angle in the laboratory frame between the velocity $\vec{v}_{1f}$ and the center-of-mass velocity $\vec{v}_{cm}$. The quantities in the center-of-mass frame are marked by an asterisk, $*$, so v^* is the speed of the particle and θ^* is the scattering angle in the center-of-mass frame. We represent the uniform distribution of $\cos\theta^*$ in the range $[-1\ 1]$ by

$$\cos\theta^* = 1 - 2r, \tag{3}$$

where random numbers r are uniformly distributed in the range $[0\ 1]$. For our monoenergic ($v_1 = v_2 = v$) case, the quantities are: $\sqrt{2}v_{cm} = v\sqrt{1+\cos\theta_{12}}$, and $\sqrt{2}v^* = v\sqrt{1-\cos\theta_{12}}$, where θ_{12} is the collision angle between the velocity vectors $\vec{v_1}$ and $\vec{v_2}$. Therefore, the equations are simplified; in particular

$$\cos\theta_{1f} = \frac{\sqrt{1+\cos\theta_{12}} + \cos\theta^*\sqrt{1-\cos\theta_{12}}}{\sqrt{2}\sqrt{1+\cos\theta^*\sin\theta_{12}}} \tag{4}$$

and

$$\cos\theta_{2f} = \frac{\sqrt{1+\cos\theta_{12}} - \cos\theta^*\sqrt{1-\cos\theta_{12}}}{\sqrt{2}\sqrt{1-\cos\theta^*\sin\theta_{12}}}. \tag{5}$$

These equations, Eq. 4 and 5, together with an assumed uniform spatial distribution of vectors $\vec{v}_{cm}$, serve as the basis for the numerical analysis of the coincidence probability. First, from inspection of Eq. 4 and 5 it can be shown that for collision angles $\theta_{12} < 90°$, the final velocities, $\vec{v}_{1f}$ and $\vec{v}_{2f}$ are always directed at acute angles to $\vec{v}_{cm}$. For example, Fig. 3 shows θ_{1f} and θ_{2f} for $\theta_{12} = 85°$. For such a case both outgoing neutrons are directed into the same hemisphere with respect to the center-mass velocity vector and therefore no coincidence is possible.

For collision angles $\theta_{12} > 90°$ the final velocity vectors are directed at obtuse angles to $\vec{v}_{cm}$, so detector coincidences are possible but only if two conditions are fulfilled simultaneously: 1) the vector $\vec{v}_{cm}$ lies along the z-axis inside $\Delta\Omega_{det}$ and 2) the corresponding angles θ_{1f}, θ_{2f}, of the two final velocity vectors are about $0°$ and $180°$ within the range of $\theta_{det} \approx 1°$. Fig. 4 presents plots θ_{1f} and θ_{2f} as a function of θ^* for different values of obtuse θ_{12} angles. The coincidences are possible for θ^* near zero, which rarely happens.

Since $\Delta\Omega_{det}$ is defined as the relative solid angle, it also gives the probability for meeting the first condition above, that is when the vector $\vec{v}_{cm}$ lies along the z-axis inside $\Delta\Omega_{det}$. The probability governing the second condition is determined from the range of random numbers, Δr, in Eq. 3, which describes the isotropic scattering in the center-of-mass frame. Therefore, if the total number of collisions inside the YAGUAR through-channel is N_{nn}, then the number of two-detector coincident counts is

$$N^{det}_{coinc} = 2 \times N_{nn} \times \Delta\Omega_{det} \times \Delta r, \tag{6}$$

while the number of single detector counts [7] is given by

$$N^{det}_{single} = 2 \times N_{nn} \times \Delta\Omega_{det}, \tag{7}$$

which leads us to the final estimate of the probability of coincidences relative to the single detector counts,

$$P_{coinc} = \Delta r. \tag{8}$$

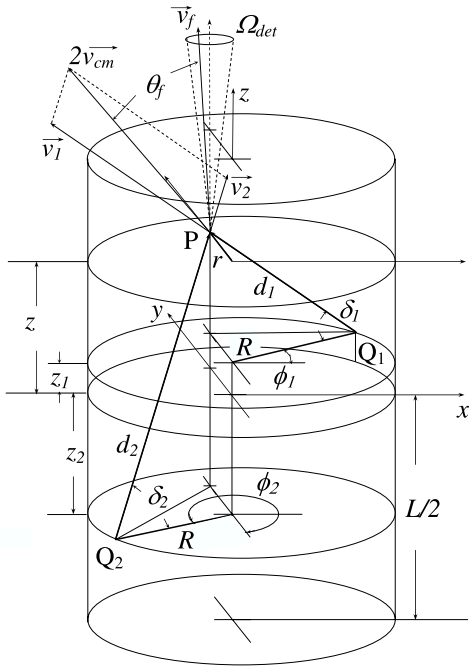

Figure 2: Diagram of scattering geometry. Neutrons leaving source points Q_1 and Q_2 on the internal surface of the neutron moderator (not shown), collide at point P, with initial velocities $\vec{v}_1$ and $\vec{v}_1$ and the collision angle θ_{12}. Final velocities in the laboratory frame, $\vec{v}_{1f}$ and $\vec{v}_{2f}$ make angles θ_{1f} and θ_{2f} with the center-of-mass velocity $\vec{v}_{cm}$.

By applying Eq. 4 and 5, we find that condition 2) is fulfilled nearly independent of the obtuse θ_{12} values, for the range of random numbers r in the interval $[0 \;\; 7.6 \times 10^{-5}]$ while the total range of r for all possible scattering angles θ^* is $[0 \;\; 1]$. Therefore, our analytical estimate for two-detector coincidences if $P_{coinc} \approx 0.8 \times 10^{-4}$. This value is an upper limit because it does not include the collimation system or the time-of-flight window which would further reduce the expected coincidence rate.

3 Monte-Carlo modeling with code PZSIM

In order to investigate the coincidence rate with the full geometry and the neutron energy distribution, we modified the PZSIM (**P**roduction in **Z SIM**ulation) code used to model the nn-experiment in [1] to include a second detector of either 20 cm or 200 cm diameter placed 12 m above the reactor, mirroring the placement of the original 20-cm diameter detector 12 m below the reactor. No collimators were assumed for the upper detector, but the same simplified collimation system used in [1] and shown in Fig. 1 was assumed for the main detector. As explained in [1] the PZSIM code uses the Amaldi analytical expressions for the scattering kinematics [9]. The code chooses a collision point within the scattering volume (YAGUAR through channel), chooses neutron starting positions along the internal wall of the cylindrical moderator, and chooses energies from a Maxwellian distribution with an epithermal tail. Based on the initial trajectories, the velocities are transformed to the center-of-mass system where scattering is isotropic. The new velocities

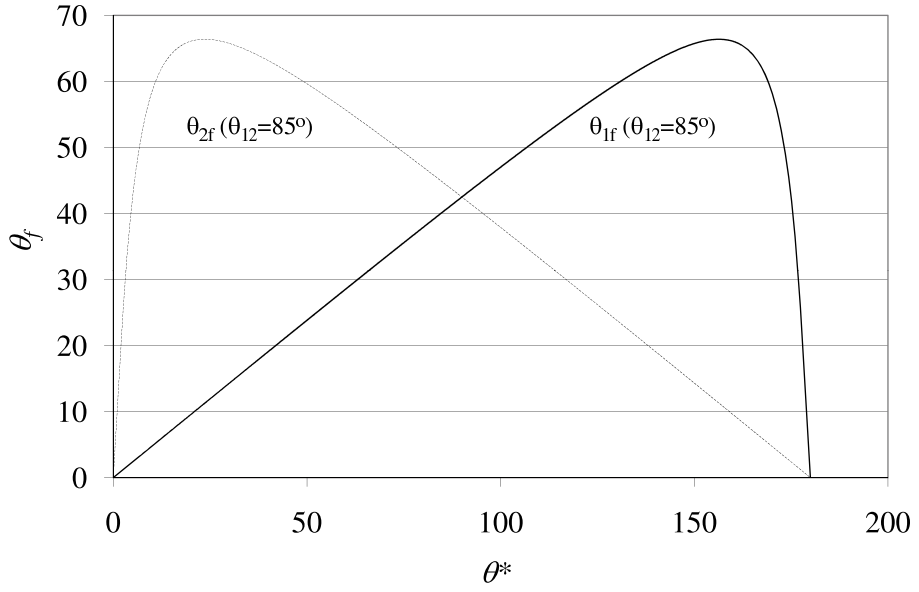

Figure 3: Plot of θ_{1f} (dark line) and θ_{2f} (light line) for $\theta_{12} = 85°$. For any $\theta_{12} = 85°$ the angles θ_{1f} and θ_{2f} are both in the same hemisphere with respect to the center-mass velocity vector. Therefore, coincidence counts in opposite detectors are impossible.

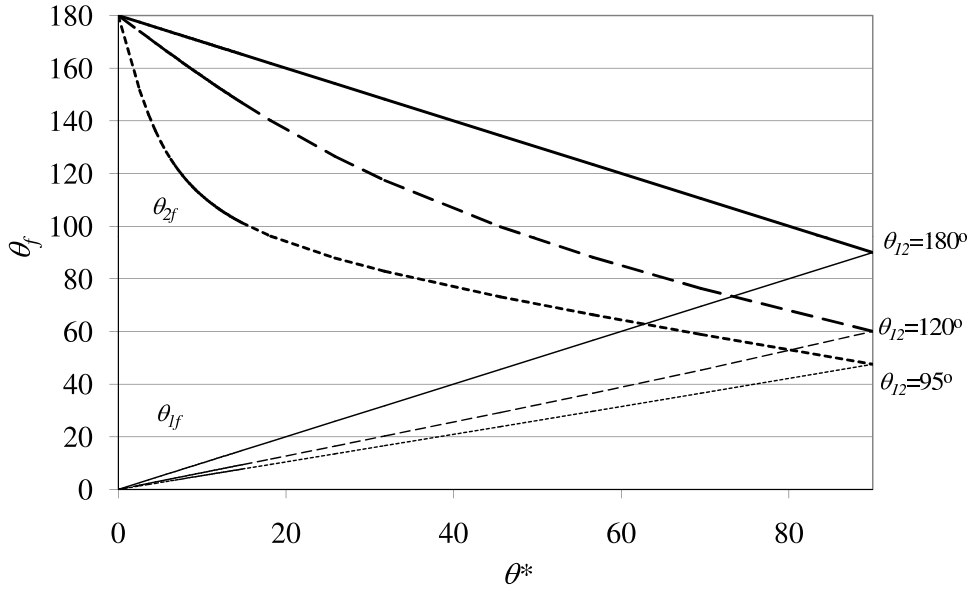

Figure 4: Plot of final angles with respect to the center-of-mass velocity, θ_{1f} (upper light lines) and θ_{2f} (lower dark lines), as a function of θ^* for different scattering angles, θ_{12}. Coincidence counts are possible. However, for the YAGUAR geometry as dicussed in the text, θ_{1f} must be within about 1° of 0° and θ_{2f} must be within about 1° of 180°. This rarely occurs.

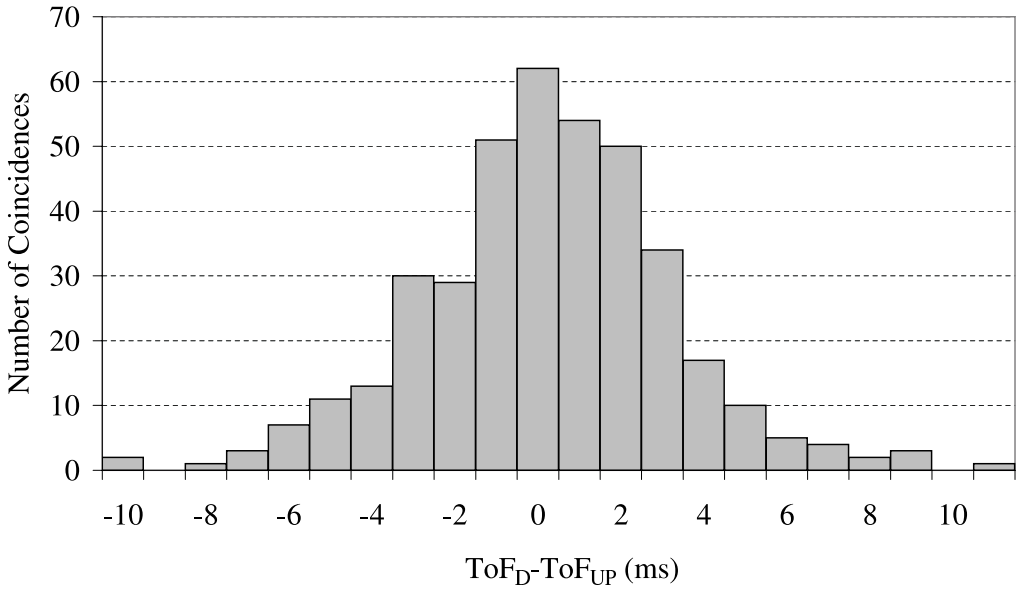

Figure 5: Histogram of the difference between arrival time-of-flight at the main detector and the upper detector for the case of a 200-cm upper detector and 20-cm main detector. There were 398 coincidences out of 1.4×10^6 main detector hits.

of both neutrons after scattering are transformed back to the laboratory frame by adding the center-mass velocity vector. Each neutron is then followed along its path until it collides with the moderator wall, a collimator, or the detectors.

Running the modified PZSIM code with a 20-cm diameter upper detector we find that only a few of the 10^6 neutrons which reach the main, bottom detector have a partner that makes it to the second, top detector at *any* time of flight, though the statistics of this result are quite poor. To improve the statistics the upper detector by a factor of 100, the diameter of the detector was increased to 200 cm. The coincidence rate for this rather large detector is 3×10^{-4} of the main detector count rate. Scaling this result down to the more reasonable detector size of 20 cm in diameter, we get 3×10^{-6}. This result is quite reasonable when one considers the fact that not only do most neutrons collide with the moderator walls, but also the vast majority (98% in our simulation) of neutrons that reach the main detector originate from a collision between two neutrons that happen to both be traveling with their initial z-component of velocity towards the main detector.

The reality of time-of-flight is not included in the above coincidence probability. Of the very small fraction of detector counts that have a coincidence partner reaching the other detector, the time-of-flight for the two neutrons can vary drastically given the wide range of neutron energies involved in the collisions. The time-of-flight for the coincidences range over ~ 10 ms (which corresponds with the time-of-flight interval of the Maxwellian spectrum), as shown in Fig. 4. By limiting the coincidence window to 1 ms, the overall probability for coincidences is $< 10^{-6}$.

4 Conclusion

We conclude that the coincidence rate in a hypothetical two-detector YAGUAR nn-experiment is far too low to be of any pratical use in the direct measurement of the nn-singlet scattering length. The main reason for such a small effect is the conservation of energy and momentum in the interaction between two particles of equal mass. Even though the particles go in opposite directions in the center-of-mass frame, only relatively rare head-on collisions with the center-of-mass velocity close to zero are relevant for coincidences in the lab frame. An additional reason for the low coincidence rate is the wide dispersion of neutron arrival times to the two detectors due to the broad thermal energy spectral range.

5 Acknowledgments

This work was supported in part by the International Science and Technology Center under project No. 2286, the Russian Foundation for Basic Research Grant No. 05-02-17636, and the US National Science Foundation Low Energy Nuclear Science RUI Award No. 0555652.

References

[1] B. E. Crawford *et al.*, J. Phys. G: Nucl. Part. Phys. **30** (2004) 1269.
[2] Slaus I., *et al.*, Physics Reports **173**, No. 5 (1989) 257.
[3] C. R. Howell *et al.*, Phys. Lett. B **444** (1998) 252.
[4] D. E. González Trotter *et al.*, Phys. Rev. C **73** (2006) 034001.
[5] V. Huhn, *et al.*, Nuclear Physics A **684** (2001) 632.
[6] B.G. Levakov, *et al.*, Physics, Safety and Applications of Pulsed Reactors, Washington DC (1994) 67.
[7] W. I. Furman, *et al.*, J. Phys. G: Nucl. Part. Phys. **28** (2002) 2627.
[8] Muzichka, A. Yu., *et al.*, Nucl. Phys. A **789** (2007) 30.
[9] E. Amaldi, in: S. Flügge, (Ed.), Handbuch der Physik, XXXVIII/2, Springer-Verlag, Berlin, 1959, p.1.